Hindawi
Complexity
Volume 2023, Article ID 4977217, 12 pages
https://doi.org/10.1155/2023/4977217

Research Article

Transient Dynamics of a Food Chain Model with Vigilance in the Biparameter Spaces

Min Wu

Publicity Office of the CPC TFSU Committee (News Center), Tianjin Foreign Studies University, Tianjin 300204, China

Correspondence should be addressed to Min Wu; wumin@tjfsu.edu.cn

Received 19 September 2023; Revised 9 December 2023; Accepted 15 December 2023; Published 31 December 2023

Academic Editor: Daniel Oro

This article focuses on the asymptotic and transient behavior of a food chain model with vigilance in the biparameter spaces. Firstly, the local asymptotic stability conditions of the positive equilibrium point are obtained. Then, the transient dynamical behavior of the positive equilibrium point is analyzed based on eight parameters. Using numerical simulation, the stable regions of the model with single and double parameters are plotted, as well as the value changes of resilience, reactivity, and amplification envelope within the stable regions. The results show that the coexistence equilibrium point is always reactive, and the corresponding parameter ranges for system stability are large, but the resilience values are small. The vigilance parameter of the middle- and lower-level organisms has the greatest impact on the system's resilience and reactivity, and the lowest vigilance corresponds to the maximum resilience and reactivity. Our results provide important references for effective management and protection of wild animal populations by the potential for transient amplification, disturbance growth time, and amplitude.

1. Introduction

Ecological theory has always focused on long-term or asymptotic behavior as a way of understanding natural systems, and the equilibrium of ecological models is typically characterized by their stability and resilience. In 1977, Pimm and Lawton [1] first proposed the biological concept of resilience, which refers to the asymptotic decay rate of perturbations, and concluded that "the greater the resilience, the faster the long-term decay rate of perturbations, and the more stable the system." As a result, the asymptotic behavior of the solution of a linearized system can be described by the dominant eigenvalue. However, ecological systems with asymptotically stable equilibria may exhibit deviations from equilibrium in the short term after disturbances. Therefore, Neubert and Caswell [2] introduced reactivity and amplification envelopes as supplements to resilience in 1997, to explain why perturbations can grow significantly before decaying, opening up a path for the analysis of nonpattern stability in ecological problems.

People gradually realized that these short-term dynamics, or transients, may differ. In 2001, Chen and Cohen [3] showed that transients are one of the important factors affecting the sustainability of ecological communities. Hastings [4] also proposed that transients are a key to understanding long-term ecology in 2004. In the same year, Neubert et al. [5] studied the reactivity of predator-prey and food web models and concluded that coexistence equilibria are reactive in all predator-prey and food web models, and short-term disturbances amplified the real possibility of predator-prey interactions and food webs. Caswell and Neubert [6] also focused on the short-term dynamics of long-term stable reactive ecological systems and studied the reactivity of discrete-time predator-prey models and density-dependent matrix population models in 2005, concluding that reactivity is common (but not universal).

More and more scholars have found that the transient growth of disturbances is a key attribute of dynamic behavior in ecological systems. Many studies have also focused on understanding the ecological reasons for transient growth of disturbances (Verdy and Caswell [7], Snyder [8]) and developing a theoretical framework (Neubert et al. [9]) for identifying transient growth in ecological time series obtained from experiments. In 2014, Tang and Allesina [10]

derived analytical standards for the reactive behavior of large ecological systems with species random interactions. The latest advances in understanding the transient dynamics of complex ecological systems have revealed that transients can also persist for relatively long periods of time. Hastings et al. [11] systematically defined "long-term transients" in 2018, pointing out that long transients have two characteristics: a long duration of quasistable state and a short time for regime shift, and proposed ghosts and crawl-bys as its core mechanism. Long-term transient dynamics can easily be mistaken for stable state dynamics but may require radically different management strategies. In 2020, Boettiger [12] explored the optimal management of stochastic ecological systems with long-term transients. Morozov et al. [13] also quantitatively analyzed this important feature in ecology "long-term transients" in the same year and conducted systematic research, revealing several major mechanisms that lead to the appearance of long transients, filling the gap in the study of ecological transients and providing a deeper understanding of the stability and sustainability of ecological systems. In 2023, Sahoo and Samanta [14] explored the impact of fear and its legacy effects on long-transient dynamics.

Reactivity has been extensively studied in many two-dimensional ecological models, such as ecosystem compartment models (Marvier et al. [15]), two-dimensional infectious disease models (Hosack et al. [16]), and matrix population models (Ezard et al. [17]). In 2017, Vesipa and Ridolfi [18] demonstrated the significant dynamic impact of seasonal forcing on a predator-prey model with a Holling II type functional response. Considering that ecological systems are constantly influenced by external factors in the real world, it is reasonable to consider stochastic biological models. In 2014, Buckwar and Kelly [19] extended resilience, reactivity, and other quantitative standards to perturbed predator-prey models with stochasticity. In 2021, Liu and Feng [20] measured how three quantitative standards (mean-square resilience, mean-square reactivity, and mean-square amplification envelope) change under different perturbation conditions using a stochastic proportional dependence predator-prey model as an example. In the same year, Sahoo et al. [21] investigated the interplay between the level of fear and the degree of habitat complexity in a predator-prey model with two different shaped functional responses.

With the development of mathematics, community models based solely on two species as basic components may overlook important ecological behaviors. In 1973, Rosenzweig [22] and, in 1976, Wollkind [23] discovered complex and striking results in a three-nutrient level model, far beyond what was seen in the two-species model. In 1987, Fretwell [24] proposed that food chain dynamics are the core theory of ecology. In 2019, Panday et al. [25] introduced the concept of fear cost into a three-species food chain model and found that it could stabilize a system that was previously in constant fluctuation. Cong et al. [26] established a three-species food chain model in 2021 that included antipredator behavior costs and benefits, which also confirmed the above theory. In 2022, Hossain et al. [27] studied the changes in population density in different bivariate spaces of a three-species food chain model with a vigilant component and found that vigilance plays a crucial role in the survival and extinction of populations. In 2023, Mandal et al. [28] explored the effects of predator fear and supplementary food sources on interacting populations in a three-nutrient food chain model.

Although the asymptotic stability of food chain models has been well established, there has been relatively little research on transient behavior. This paper focuses on a three-species food chain model with a vigilant component, and the asymptotic and transient behaviors of the system in single and bivariate parameter spaces, including the basal prey vigilance, birth rate, mortality, and intermediate predator vigilance, et al. are investigated.

The structure of this paper is as follows: Section 2 provides a brief introduction to a mathematical model and related basic concepts. Subsequently, Section 3 obtains the local asymptotic stability conditions and parameter stability range of the model. Section 4 uses numerical simulations to obtain numerical graphs of resilience, reactivity, and amplification envelope under single and bivariate parameter perturbations and provides corresponding analysis.

2. Preliminaries

2.1. The Mathematical Model. Huang and Sih [29] studied a three-dimensional food chain consisting of green sunfish, smallmouth salamander larvae, and hatchery isopods. After documenting the negative impacts of the top predator, green sunfish, on the intermediate predator, salamanders, and the salamanders' impacts on the isopods that served as bait, they found that the fish caused the salamanders to become dramatically less active and eat less (even when the salamanders were in the same refuges as the isopods). Similarly, in response to the risk of predation, isopods increased their tendency to bury themselves in deeper sand. For this reason, we considered a three-species food chain model [30]:

$$\begin{aligned}\frac{\mathrm{d}x}{\mathrm{d}t} &= (r - m_1)x - cx^2 - P_1xy,\\ \frac{\mathrm{d}y}{\mathrm{d}t} &= d_1P_1xy - Q_1yz - m_2y,\\ \frac{\mathrm{d}z}{\mathrm{d}t} &= d_2Q_1yz - m_3z.\end{aligned} \tag{1}$$

Here, x, y, and z, respectively, denote the population size of the prey, middle predator, and top predator species. t denotes time, and m_1, m_2, and m_3 represent the natural death rates of prey, middle predator, and top predator, respectively. r is the birth rate of the prey, and c is the strength of intraspecific competition among prey individuals. d_1 and d_2 are the conversion efficiencies of preys' biomass into middle predators' biomass and middle predators' biomass into top predators' biomass, respectively. P_1 and Q_1 are the maximum predation rates of middle and top predators, respectively. The maximum predation rate of an arbitrary predator can be viewed as (the maximum

encounter rate) × (lethality) of the predator. Our main objective is to study the effect of a biparameter variation of the food chain model with vigilance on the dynamical behavior of this system. We assume that the alerting effect of the basal prey produces two effects:

(i) Due to increased vigilance, the reduced foraging time and food intake have weakened the activities that promote population growth, resulting in a decline in the birth rate of x.

(ii) Increased vigilance reduces successful predator attacks, as the basal prey has more time to hide or flee from dangerous sources, resulting in lower maximum encounter rates and catch-lethality of middle predators against basal prey. Thus, the vigilance of basal prey reduces the maximum predation rate of middle predators.

Similarly, the heightened vigilance of intermediate predators reduces their hunting time, lowers their maximum encounter rate with top predators, and thus decreases their maximum encounter rate with basal prey and maximum predation rate with top predators. The improved model is as follows:

$$\begin{aligned}\frac{\mathrm{d}x}{\mathrm{d}t} &= rx(1-u) - m_1 x - cx^2 - \frac{pxy(1-v)}{l_1 + k_1 u},\\ \frac{\mathrm{d}y}{\mathrm{d}t} &= \frac{d_1 pxy(1-v)}{l_1 + k_1 u} - \frac{qyz}{l_2 + k_2 v} - m_2 y,\\ \frac{\mathrm{d}z}{\mathrm{d}t} &= \frac{d_2 qyz}{l_2 + k_2 v} - m_3 z.\end{aligned} \tag{2}$$

The interpretations of the system parameters along with their dimensions are given in Table 1. Note that all the system parameters must be non-negative.

2.2. Measurements of Perturbation Response. Table 2 gives the measures of the response of a linear or linearized system ($\dot{x} = Ax$) to perturbations ($x(0) = x_0$) of the asymptotically stable equilibrium ($x = 0$).

3. Local Stability Analysis of Positive Equilibrium Points

This system has four equilibrium points: $E_0(0, 0, 0)$, $E_1(r(1-u) - m_1/c, 0, 0)$, $E_2(m_2(l_1 + k_1 u)/d_1 \quad p(1-v), l_1 + k_1 u/p(1-v)[r(1-u) - m_1 - cm_2(l_1 + k_1 u)/d_1 p(1-v)], 0)$, and $E^*(x^*, y^*, z^*)$. After calculation, we can obtain

$$\begin{aligned}x^* &= \frac{1}{c}\left[r(1-u) - m_1 - \frac{py^*(1-v)}{l_1 + k_1 u}\right],\\ y^* &= \frac{m_3(l_2 + k_2 v)}{d_2 q},\\ z^* &= \frac{l_2 + k_2 v}{q}\left[\frac{d_1 px^*(1-v)}{l_1 + k_1 u} - m_2\right].\end{aligned} \tag{3}$$

Here, we consider only the coexistence equilibrium point in the biological sense and its local asymptotic stability conditions.

Theorem 1. *If* $r(1-u) > m_1 + cm_2(l_1 + k_1 u)/d_1 p(1-v) + p(1-v)m_3(l_2 + k_2 v)/d_2 q(l_1 + k_1 u)$, *the interior equilibrium point* $E^*(x^*, y^*, z^*)$ *is locally asymptotically stable.*

Proof. Linearize the system (2) at $E^*(x^*, y^*, z^*)$ and obtain the Jacobian matrix:

$$\begin{pmatrix} -cx^* & -\dfrac{px^*(1-v)}{l_1 + k_1 u} & 0\\ \dfrac{d_1 py^*(1-v)}{l_1 + k_1 u} & 0 & -\dfrac{m_3}{d_2}\\ 0 & \dfrac{d_1 d_2 px^*(1-v)}{l_1 + k_1 u} - d_2 m_2 & 0 \end{pmatrix}, \tag{4}$$

its characteristic equation is $f(\lambda) = \lambda^3 + n_1\lambda^2 + n_2\lambda + n_3$, where

$$\begin{aligned}n_1 &= cx^* > 0,\\ n_2 &= \frac{d_1 m_3 px^*(1-v)}{l_1 + k_1 u} + \frac{d_1 p^2 x^* y^*(1-v)^2}{(l_1 + k_1 u)^2} - m_2 m_3,\\ n_3 &= \frac{d_1 pcm_3(x^*)^2(1-v)}{l_1 + k_1 u} - m_2 m_3 cx^*\\ &= r(1-u) - m_1 - \frac{cm_2(l_1 + k_1 u)}{d_1 p(1-v)} - \frac{p(1-v)m_3(l_2 + k_2 v)}{d_2 q(l_1 + k_1 u)} > 0,\\ M &= n_1 n_2 - n_3\\ &= cx^*\left(\frac{d_1 m_3 px^*(1-v)}{l_1 + k_1 u} + \frac{d_1 p^2 x^* y^*(1-v)^2}{(l_1 + k_1 u)^2} - m_2 m_3\right)\\ &\quad - \frac{d_1 pcm_3(x^*)^2(1-v)}{l_1 + k_1 u} + m_2 m_3 cx^*\\ &= \frac{cd_1 p^2(x^*)^2 y^*(1-v)^2}{(l_1 + k_1 u)^2} > 0.\end{aligned} \tag{5}$$

The Routh – Hurwitz conditions are satisfied, the real part of all eigenvalues of $J(E^*)$ is negative, and the positive equilibrium point E^* is locally asymptotically stable. □

4. Numerical Simulation and Stability Analysis

First, we use the following set of biologically feasible parameters:

$r = 2$, $c = 0.1$, $p = 0.7$, $q = 0.5$, $u = 0.5$, $v = 0.6$, $k_1 = 1.5$, $k_2 = 1.8$, $d_1 = 0.5$, $d_2 = 0.7$, $m_1 = 0.3$, $m_2 = 0.1$, $m_3 = 0.05$, $l_1 = 1.2$, and $l_2 = 1.5$.

Table 1: Details about the variables and parameters present in system (2) [31].

Parameter	Dimension	Interpretation
t	Time	Time
x	Biomass	Basal prey's density
y	Biomass	Intermediate predator's density
z	Biomass	Top predator's density
r	Time^{-1}	Birth rate of the basal prey
m_1	Time^{-1}	Natural death rate of the basal prey
m_2	Time^{-1}	Natural death rate of the middle predator
m_3	Time^{-1}	Natural death rate of the top predator
c	Time^{-1} biomass^{-1}	Intraspecific competition rate of the basal prey
p	Time^{-1} biomass^{-1}	Maximum predation rate of middle predator
q	Time^{-1} biomass^{-1}	Maximum predation rate of top predator
d_1	Dimensionless	Conversion efficiency of the middle predator
d_2	Dimensionless	Conversion efficiency of the top predator
$1/l_1$	Dimensionless	Middle predator's lethality
$1/l_2$	Dimensionless	Top predator's lethality
u	Dimensionless	Level of vigilance of the basal prey
v	Dimensionless	Level of vigilance of the middle predator
k_1	Dimensionless	Effectiveness of basal prey's vigilance
k_2	Dimensionless	Effectiveness of middle predator's vigilance

Table 2: Measurements of perturbation response [2].

Quantity	Definition	Calculation method
Resilience	Asymptotic proportional decay rate of perturbations: $\lim_{t\to\infty}(1/\|x(t)\|d\|x(t)\|/\mathrm{d}t)$	$-\mathrm{Re}(\lambda_1(A))$
Reactivity	Maximum possible instantaneous proportional amplification rate of perturbations: $\max_{\|w_0\|\neq 0}[(1/\|x(t)\|d\|x(t)\|/\mathrm{d}t\mid_{t=0})]$	$\lambda_1(H(A))$
Amplification envelope $\rho(t)$	Maximum possible amplification at time t: $\max_{\|x_0\|\neq 0}\|x(t)\|/\|x_0\|$	$\|\|e^{At}\|\|$
$\rho_{\max}$	Maximum possible amplification:	$\max_{t\geq 0}\rho(t)$

[1]The dominant eigenvalue of A is $\lambda_1(A)$. [2]$H(A) = (A + A^T)/2$. The dominant eigenvalue of $H(A)$ is $\lambda_1(H(A))$. [3]The matrix norm $\|e^{At}\|$ can be calculated in Mathematica via "Norm[MatrixExp[$A * t$]]".

The parameter values for this set of assumptions are based on the reported values in [27]. At this point, the system has a stable coexistence equilibrium E^* (6.4708, 0.3686, 1.8812) (Figure 1). Next, we plot the stable regions of the model with single and double parameters, as well as the numerical changes in resilience, reactivity, and amplification envelope within the stable region. The numerical simulation presented here revolves around eight parameters: l_1, l_2, u, v, r, m_1, p, and q.

4.1. Transient Dynamics of Systems in Single-Parameter Space. Firstly, we analyze the changes in resilience and reactivity of the system under a single parameter variation. According to Theorem 1, the theoretical ranges of the first four parameters for which the E^* is locally asymptotically stable are $l_1 \in [0, 8.9028)$, $l_2 \in [0, 26.2548)$, $u \in [0, 0.744968)$, $v \in [0, 0.918888)$. Figure 2 shows that the range of parameters with positive resilience is consistent with the theoretical results. When a single parameter of the system changes within the above range, the system can still adjust itself to a stable state. The response of resilience to the parameters l_1, u, and v is small (with a maximum value not exceeding 0.166) and shows a monotonic decreasing trend. When l_2 changes, resilience shows a trend of increasing first and then decreasing, reaching a peak of 0.22 at $l_2 = 12.5$. In addition, the coexistence equilibrium point is reactive (reactivity >0).

Among the parameter variables we consider, l_1 and l_2 measure the killing power of intermediate and top predators, respectively. Higher values can be interpreted as lower foraging activity and vice versa. Figure 2 shows that when l_2 is at a lower level (with higher predation pressure from intermediate predators), the equilibrium biomass of the x population in the region is relatively high ([27]). As l_2 gradually increases (appropriately reducing the predation pressure of intermediate predators), the equilibrium biomass of the y population increases, and the system's resilience increases with the increase of l_2. However, when the value of l_2 is too high (greater than 12.5), the foraging activity of the z population decreases significantly, which greatly reduces the restriction on intermediate predators, as the y population maintains a low level of predation pressure on the base prey ($l_1 = 1.2$). This leads to an increase in the equilibrium biomass of intermediate predators, causing a sharp decline in the equilibrium biomass of x, and a sudden drop in the resilience shown in the figure (b).

According to Theorem 1 of the local asymptotic stability condition of E^*, the theoretically obtained stable ranges for the last four parameters are $r \in (0.984418, +\infty)$, $m_1 \in (0, 0.807791)$, $p \in (0.141447, 1)$, and $q \in (0.0471926, 1)$.

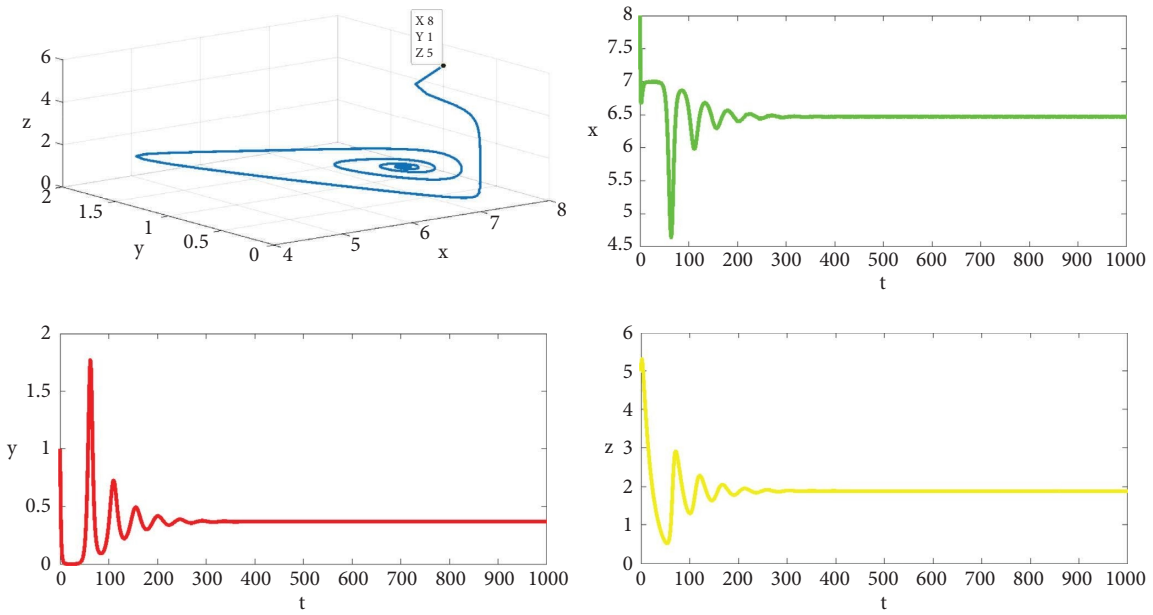

Figure 1: Phase portrait and time-series evaluations of the system (2), where the initial value is (8, 1, 5).

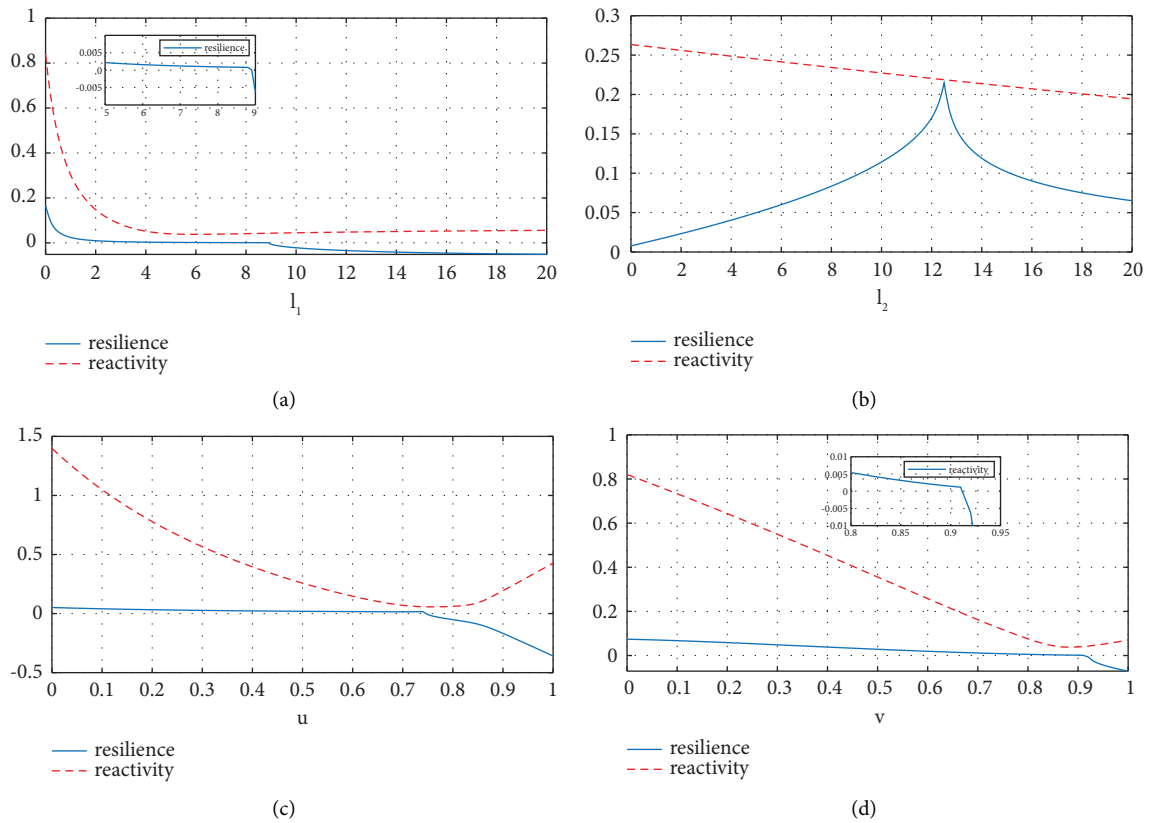

Figure 2: Resilience and reactivity as a function of the range of variation about a single parameter (l_1, l_2, u, v).

Figure 3 shows that the parameter ranges with positive resilience are consistent with the theoretical results. Resilience is not sensitive to the response of the parameters r, m_1, and p, with a maximum value not exceeding 0.04. The parameter q, which represents the attack rate of the top predator, has a minimum threshold of 0.05, and the response curve has a significant inflection point before the q value of 0.02, with a maximum peak of 0.154, followed by a decreasing trend. The coexistence equilibrium point is reactive (reactive >0).

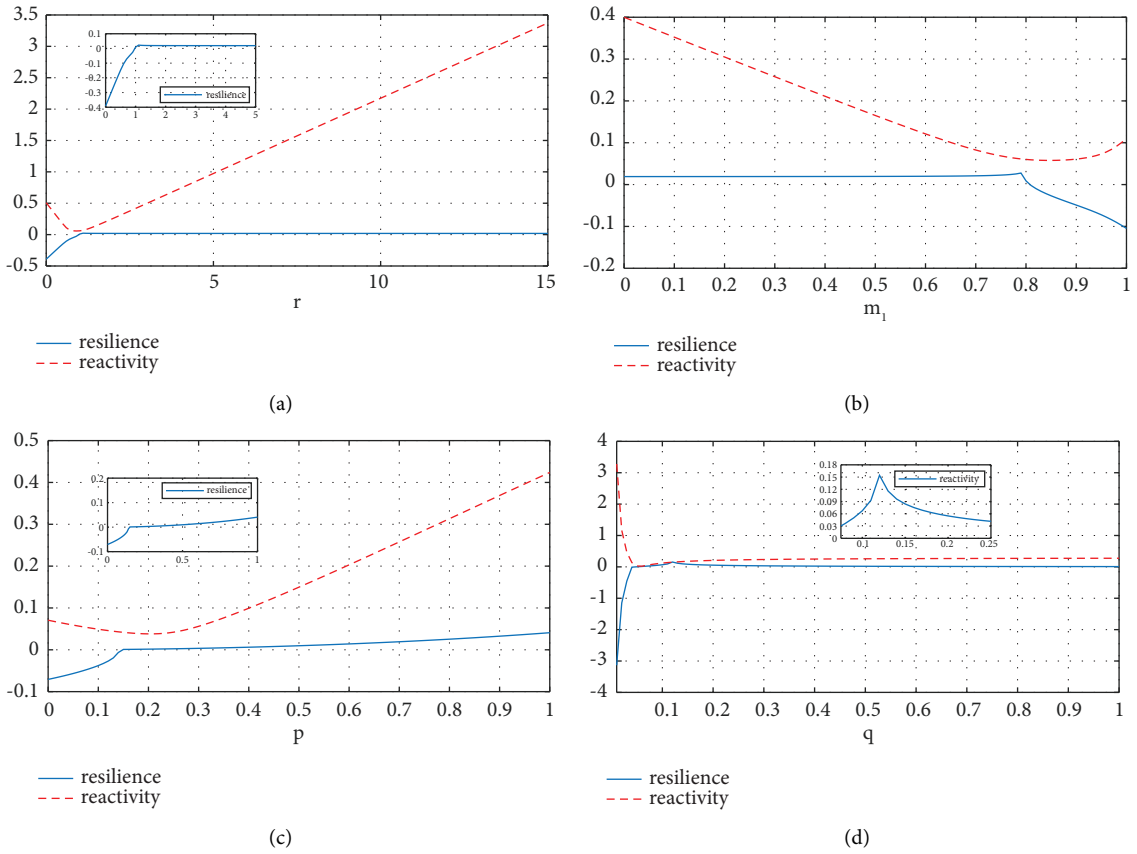

Figure 3: Resilience and reactivity as a function of the range of variation about a single parameter (r, m_1, p, q).

The range of the last four parameters for which the system is stable according to the E^* stability condition can be obtained theoretically as $r \in (0.984418, +\infty)$, $m_1 \in (0, 0.807791)$, $p \in (0.141447, 1)$, and $q \in (0.0471926, 1)$. As can be seen from Figure 3, the range in which the restoring force is positive for each parameter remains consistent with the theoretical results. The response of the restoring force to the changes of these four parameters is small, with the maximum value not exceeding 0.04, and the internal equilibrium of this system is all reactive (reactivity >0).

Figures 4–7 show the individual Figure 5 effects of Figure 6 eight parameter pairs on the amplification envelope and max (the maximum value of perturbation amplification). They provide information on the potential for disturbance growth time, amplitude, and transient amplification. We found that the impact of each parameter change on max is very consistent with its impact on reactivity. The greater the reactivity, the larger the maximum disturbance amplification $\rho_{\max}$, but there is no necessary correlation with the time it takes to return to a stable state. For example, in Figure 4, when $l_1 = 0$, the maximum value of $\rho_{\max}$ for the amplified envelope is achieved, but the time it takes to return to a stable state is the shortest.

4.2. Transient Dynamics of Systems in Biparameter Space. We have gained a rough understanding of the impact of the vigilance parameters u, v, and six other parameters on the ecosystem. However, the results only provide an isolated view of system dynamics, as they keep other parameters constant and only examine the impact of a single parameter. One major improvement of this article is to simultaneously change two parameters.

In Figure 8, figures (a) and (b) show the numerical equipotential chart of the resilience and reactivity of the system (2) within the u-$v \in [0, 1] \times [0, 1]$ bounded region. Figures (c) and (d) show the numerical equipotential chart of the resilience and reactivity of the system within the l_1-l_2 bivariate space $[0, 9] \times [0, 42]$ range. The corresponding color bars indicate the corresponding values, and the white area represents the region where the resilience is less than zero.

As seen in Figures 8(a) and 8(b), the trends of resilience and reactivity are consistent in that smaller parameter values increase asymptotic stability while also increasing transient instability, and conversely, larger parameters result in less resilience and reactivity. Ecosystem stability is highest and responsiveness to disturbance is greatest at low vigilance levels for both bottom prey and intermediate predators. Resilience and reactivity values were greatest when the vigilance parameters u and v

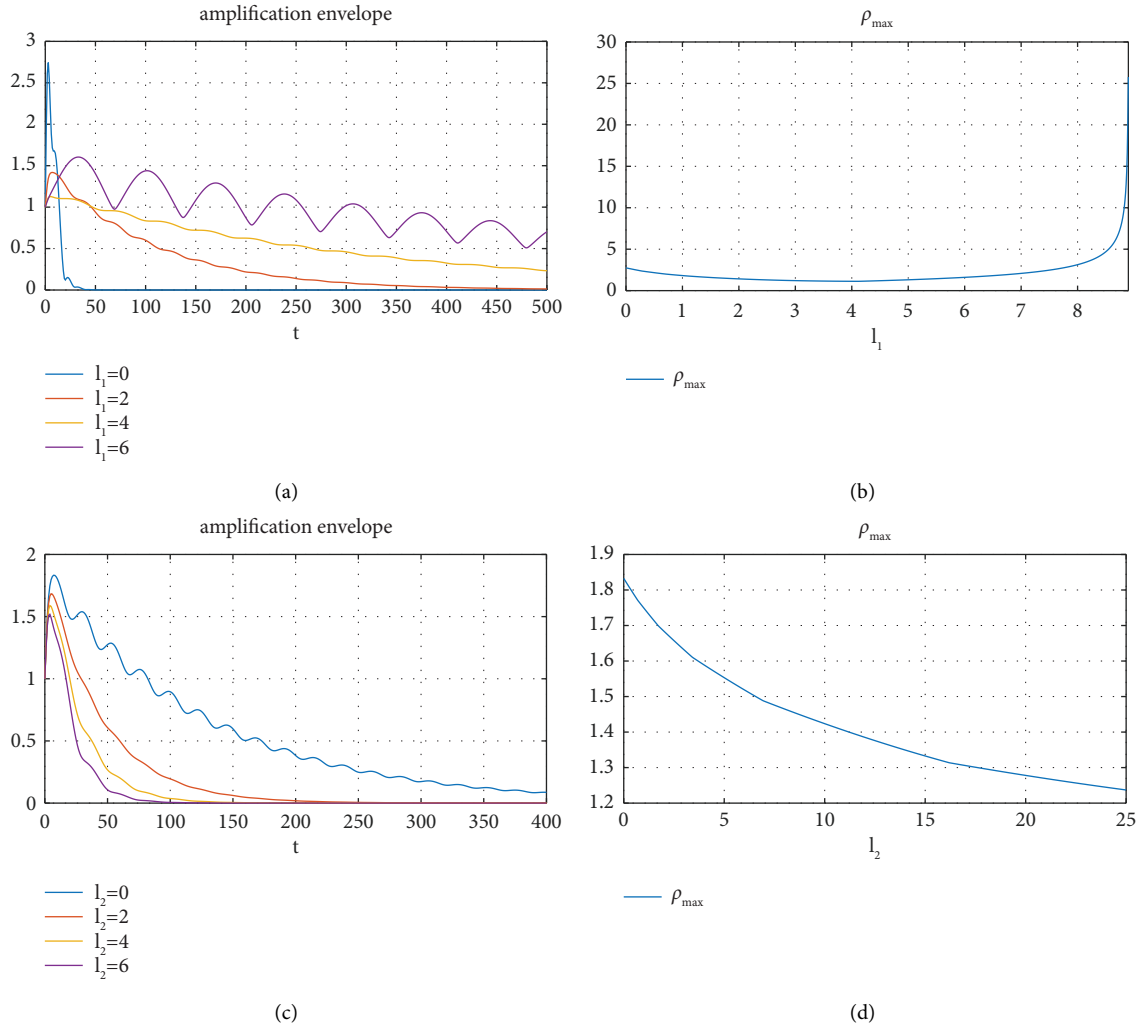

FIGURE 4: The effect of a single parameter (l_1, l_2) on the amplification envelope and $\rho_{\max}$.

were both zero. In addition, we note that the setting of u is significant for the ecosystem. When u is greater than 0.782, resilience decreases below zero regardless of the value of v. This is because u is directly related to the biomass level of the bottom prey. In the food chain, the base prey is critical for the survival of other prey.

Next, we consider the changes in resilience and reactivity in the l_1-l_2 bivariate space (Figures 8(c) and 8(d)). By observing Figures 8(c) and 8(d), we can see that the resilience has a high constraint on the range of l_1 variation, with a maximum value of 9. Moreover, most of the response regions obtained from bivariate changes have a resilience value of 0.02 and a reactivity value of 0.1. The response regions with a resilience value greater than 0.04 are concentrated around a parabolic curve, while the response regions with a reactivity value greater than 0.2 are concentrated in the lower left corner of the figure, and the maximum reactivity value corresponds to the lowest values of l_1 and l_2.

We consider another set of important parameters, r and m_1. Figures 9(a) and 9(b) show that the birth rate r of the bottom-level prey in the system must not be lower than the threshold of 0.39. When the birth rate r is below 0.39, the system resilience is less than 0 regardless of the value of m_1. When r exceeds this value, the basic prey can still be extinct from the system at a relatively high death rate under low birth rates. Overall, the impact of the biparameter variations of r and m_1 on resilience is very small, with values remaining stable at around 0.02, and the highest value being only 0.025. In Figure 9(b), the highest reactivity corresponds to high birth rates and low death rates.

The last important set of parameters, p and q, represent the attack rate (or encounter rate) of intermediate and top predators, respectively. Figures 9(c) and 9(d) show that the system only exhibits resilience and reactivity when the p value is greater than 0.143. Most of the response regions obtained from the biparameter variation show a resilience value of 0.03. In the lower right corner of Figure 9(c) ($p > 0.6$, $q < 0.3$), the maximum resilience does not exceed 0.16. By observing Figure 9(d) vertically, it can be seen that the higher the p value at the same q value, the stronger the reactivity. Although high p and q values correspond to the maximum reactivity, the numerical value is only 0.45.

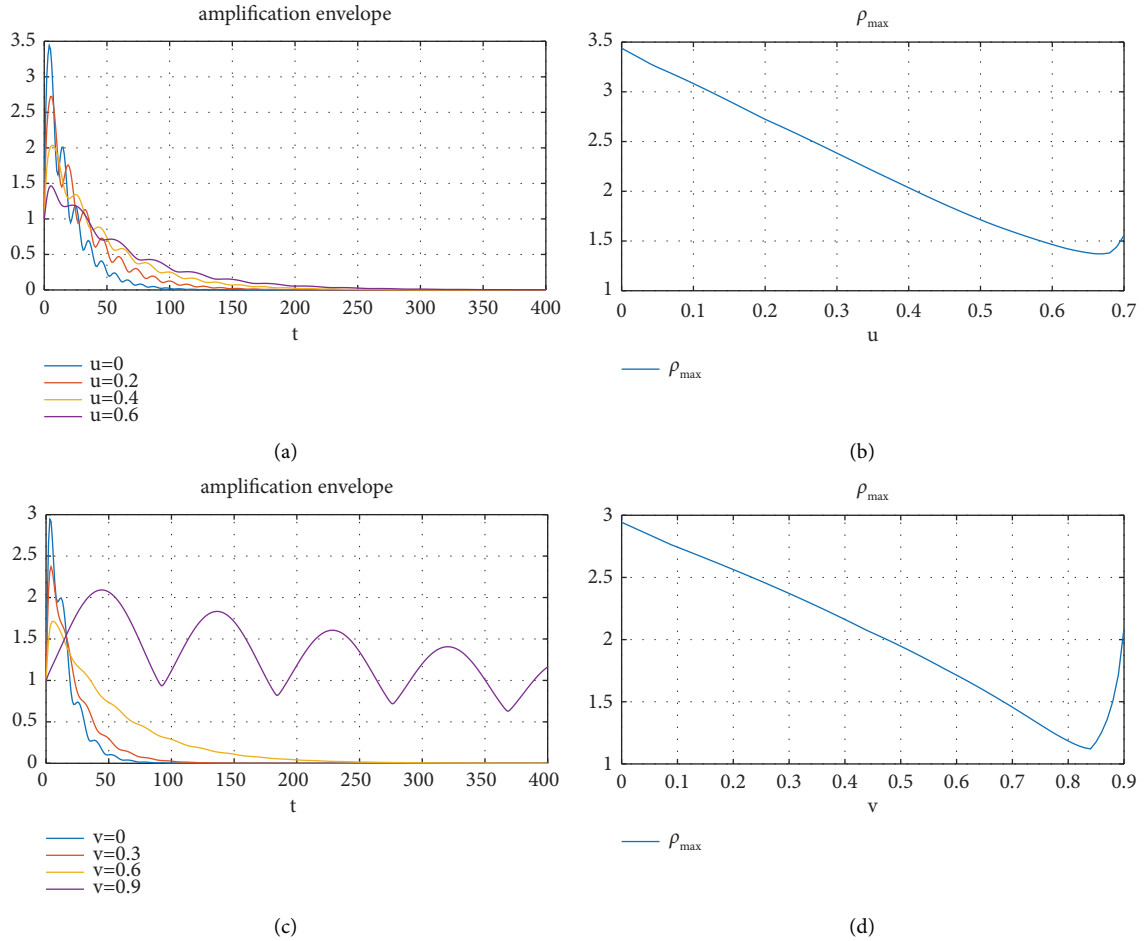

Figure 5: The effect of a single parameter (u, v) on the amplification envelope and ρ_{max}.

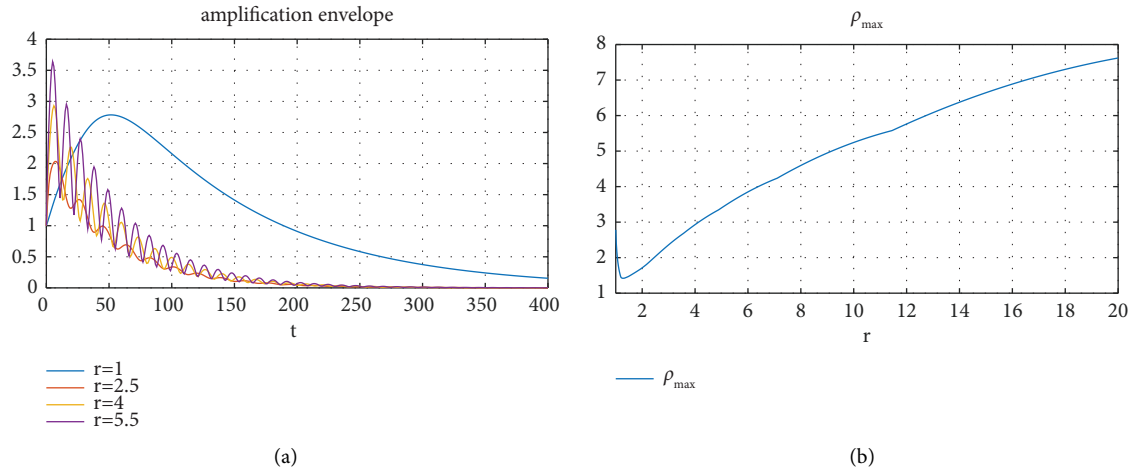

Figure 6: Continued.

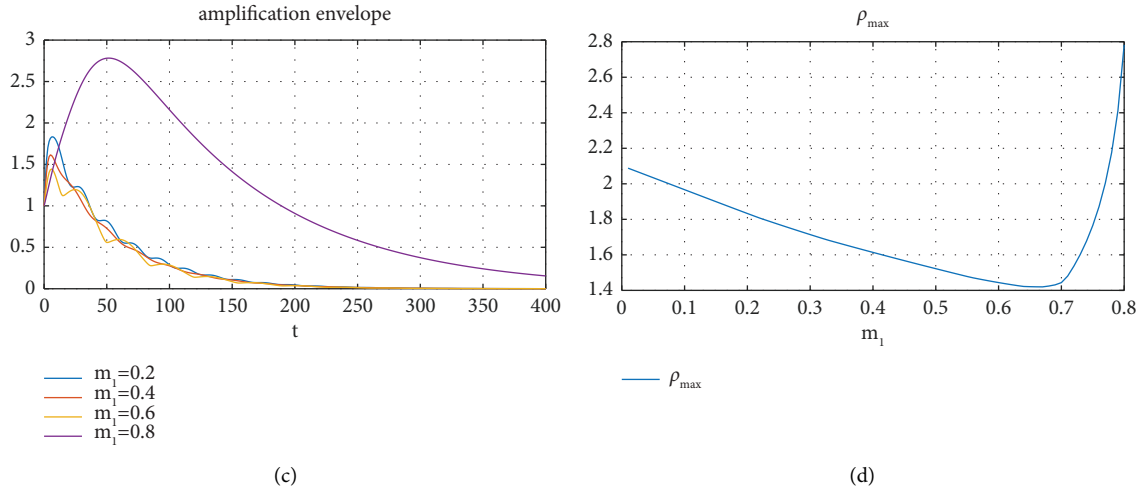

Figure 6: The effect of a single parameter (r, m_1) on the amplification envelope and $\rho_{\max}$.

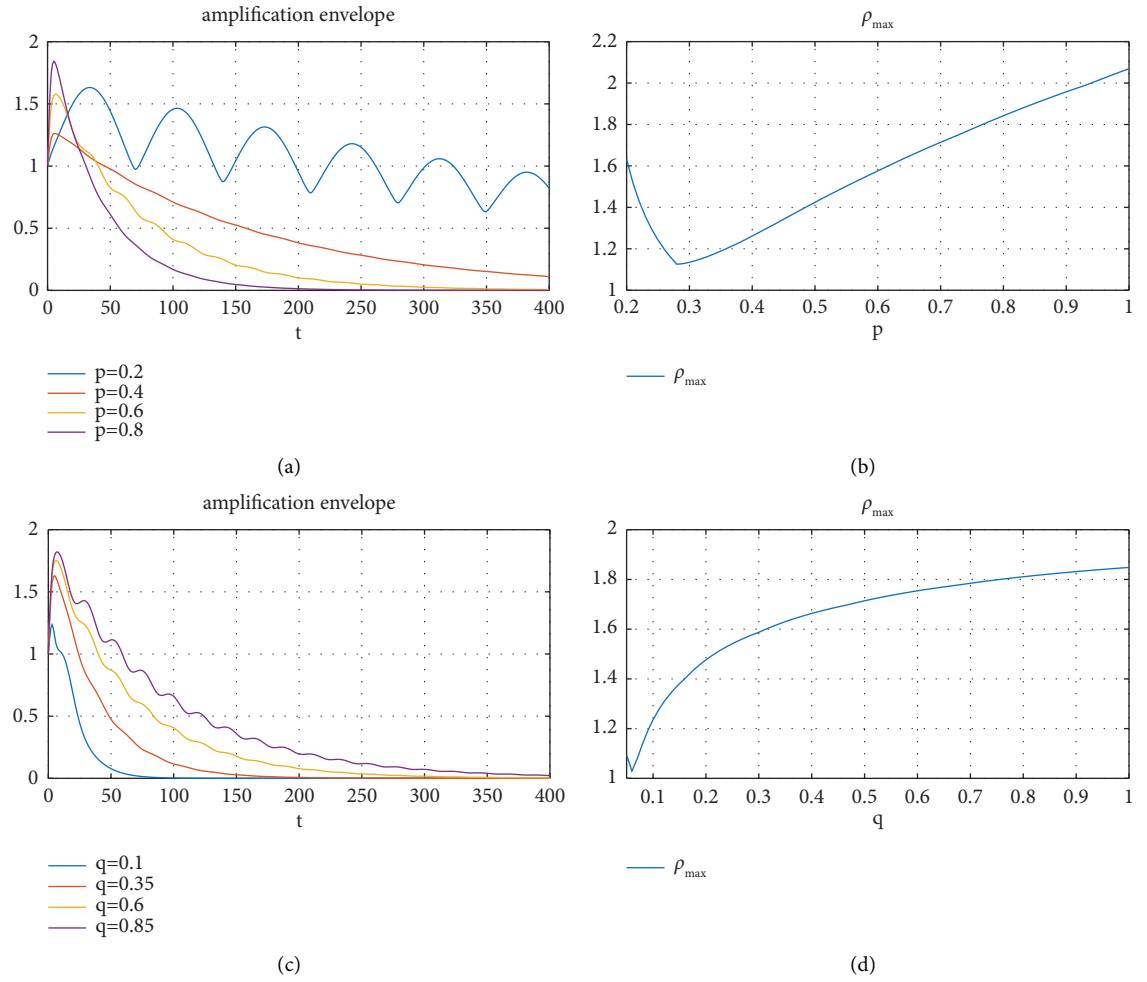

Figure 7: The effect of a single parameter (p, q) on the amplification envelope and $\rho_{\max}$.

While Hossain et al. [27] only explored the variation in population density with different parameters, we build on this by not only simulating the numerical variation in model resilience over a range of parameters desirability but also obtaining variations that indicate the transient dynamical behavior of the system, reactivity, and obtaining the maximum possible amplification of the system at time t through the amplification envelope, prompting us to take action before maximizing losses.

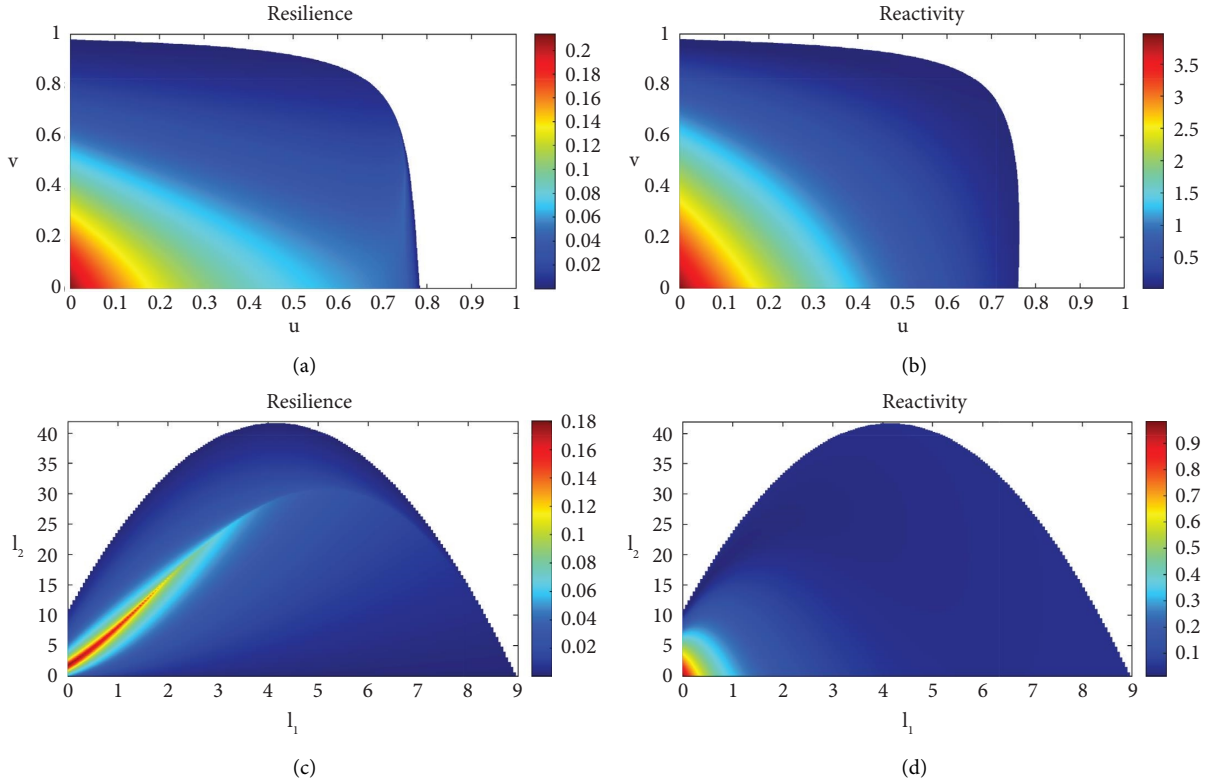

Figure 8: (a, b) The resilience and reactivity of the system within the $[0, 1] \times [0, 1]$ boundary in the u-v biparametric space. (c, d) The resilience and reactivity of the system within the $[0, 9] \times [0, 42]$ boundary in the l_1-l_2 biparametric space.

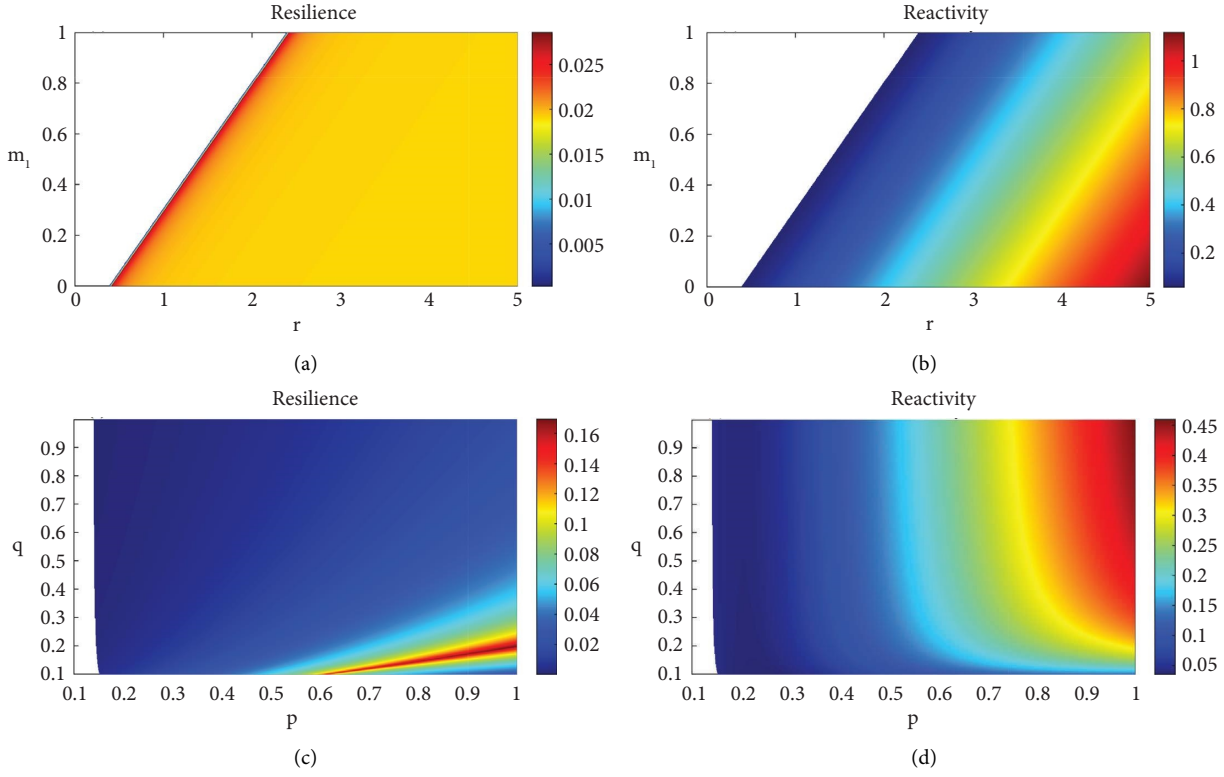

Figure 9: (a, b) The resilience and reactivity of the system within the $[0, 1] \times [0, 1]$ boundary in the p-q biparametric space. (c, d) The resilience and reactivity of the system within the $[0, 5] \times [0, 1]$ boundary in the r-m_1 biparametric space.

5. Conclusions

This article focuses on a food chain with three species that includes a vigilance factor. Eight parameters including the vigilance, birth rate, death rate of the basal prey, and the vigilance of the intermediate predator are set as single and double variables. Firstly, a single parameter variable is set and numerical simulations are used to obtain the change images of resilience, reactivity, and amplification envelope. Then, by simultaneously changing two parameters, the stable areas of the model with biparameters are plotted, and the numerical changes of resilience and reactivity within the stable regions are obtained. Based on the above analysis, this article concludes that

(1) In a single-parameter space, among the eight examined parameters, the system's resilience is most sensitive to the top predator's kill l_2 parameter, and reactivity is most sensitive to the top predator's maximum predation rate q. When regulating an ecosystem, attention should be paid to keeping parameter values within the range of the system's asymptotic stable state (with positive resilience values).

(2) In the bivariate space, the birth and mortality rates of the bottom prey r-m_1 biparameters have essentially no effect on system resilience. In contrast, the vigilance parameter of the mid-to-low level organisms has a more significant impact on both the system's resilience and reactivity. The lowest vigilance corresponds to the highest resilience and reactivity. Additionally, to ensure positive resilience, the food chain must ensure that the birth rate (r) of the lower trophic level prey and the maximum predation rate (p) of the intermediate predator are not below a certain threshold.

(3) The simulation results of the u-v bivariate space for the alertness of mid-low level organisms show a consistent trend in the changes of resilience and reactivity. That is, if the parameter changes increase asymptotic stability (by increasing resilience), it will also increase transient instability (by increasing reactivity).

(4) The coexistence equilibrium point under stable conditions is always reactive. The corresponding parameter range is large when the system is stable, but the value of resilience is small. The amplification envelope value chart provides the maximum value of disturbance amplification: $\rho_{\max}$ and the time of maximum disturbance: $t_{\max}$. Decision-makers should issue commands and actively execute them before $t_{\max}$ to avoid significant losses and save resources and manpower.

At last, as artificial interference, such as tourism, hunting, and industrial development, continues to increase, this paper provides important references for effective management and protection of wild animal populations by presenting the model's single and double parameter stable regions, as well as the numerical changes of the recovery, reactivity, and amplification envelope within the stable regions. However, we did not include noise disturbance and stochastic factors in the model. Therefore, how to deal with these factors will be an important task in future work.

Data Availability

The data used to support the findings of this study are included within the article.

Conflicts of Interest

The authors declare that they have no conflicts of interest.

References

[1] S. L. Pimm and J. H. Lawton, "Number of trophic levels in ecological communities," *Nature*, vol. 268, no. 5618, pp. 329–331, 1977.

[2] M. G. Neubert and H. Caswell, "Alternatives to resilience for measuring the responses of ecological systems to perturbations," *Ecology*, vol. 78, no. 3, pp. 653–665, 1997.

[3] X. Chen and J. E. Cohen, "Transient dynamics and food-web complexity in the Lotka-Volterra cascade model," *Proceedings of the Royal Society of London Series B Biological Sciences*, vol. 268, no. 1469, pp. 869–877, 2001.

[4] A. Hastings, "Transients: the key to long-term ecological understanding?" *Trends in Ecology and Evolution*, vol. 19, no. 1, pp. 39–45, 2004.

[5] M. G. Neubert, T. Klanjscek, and H. Caswell, "Reactivity and transient dynamics of predator-prey and food web models," *Ecological Modelling*, vol. 179, no. 1, pp. 29–38, 2004.

[6] H. Caswell and M. G. Neubert, "Reactivity and transient dynamics of discrete-time ecological systems," *Journal of Difference Equations and Applications*, vol. 11, no. 4-5, pp. 295–310, 2005.

[7] A. Verdy and H. Caswell, "Sensitivity analysis of reactive ecological dynamics," *Bulletin of Mathematical Biology*, vol. 70, no. 6, pp. 1634–1659, 2008.

[8] R. E. Snyder, "What makes ecological systems reactive?" *Theoretical Population Biology*, vol. 77, no. 4, pp. 243–249, 2010.

[9] M. G. Neubert, H. Caswell, and A. R. Solow, "Detecting reactivity," *Ecology*, vol. 90, no. 10, pp. 2683–2688, 2009.

[10] S. Tang and S. Allesina, "Reactivity and stability of large ecosystems," *Frontiers in Ecology and Evolution*, vol. 2, 2014.

[11] A. Hastings, K. C. Abbott, K. Cuddington et al., "Transient phenomena in ecology," *Science*, vol. 361, no. 6406, Article ID eaat6412, 2018.

[12] C. Boettiger, "Ecological management of stochastic systems with long transients," *Theoretical Ecology*, vol. 14, no. 4, pp. 663–671, 2020.

[13] A. Morozov, K. Abbott, K. Cuddington et al., "Long transients in ecology: theory and applications," *Physics of Life Reviews*, vol. 32, pp. 1–40, 2020.

[14] D. Sahoo and G. Samanta, "Oscillatory and transient dynamics of a slow-fast predator-prey system with fear and its carry-over effect," *Nonlinear Analysis: Real World Applications*, vol. 73, Article ID 103888, 2023.

[15] M. Marvier, P. Kareiva, and M. Neubert, "Habitat destruction, fragmentation, and disturbance promote invasion by habitat generalists in a multispecies metapopulation," *Risk Analysis*, vol. 24, no. 4, pp. 869–878, 2004.

[16] G. R. Hosack, P. A. Rossignol, and P. van den Driessche, "The control of vector-borne disease epidemics," *Journal of Theoretical Biology*, vol. 255, no. 1, pp. 16–25, 2008.
[17] T. H. G. Ezard, J. M. Bullock, H. J. Dalgleish et al., "Matrix models for a changeable world: the importance of transient dynamics in population management," *Journal of Applied Ecology*, vol. 47, no. 3, pp. 515–523, 2010.
[18] R. Vesipa and L. Ridolfi, "Impact of seasonal forcing on reactive ecological systems," *Journal of Theoretical Biology*, vol. 419, pp. 23–35, 2017.
[19] E. Buckwar and C. Kelly, "Asymptotic and transient mean-square properties of stochastic systems arising in ecology. fluid dynamics,and system control," *SIAM Journal on Applied Mathematics*, vol. 74, no. 2, pp. 411–433, 2014.
[20] W. Liu and J. Feng, "Analysis of asymptotic and transient behaviors of stochastic ratio-dependent predator-prey model," *Mathematics*, vol. 9, no. 21, p. 2776, 2021.
[21] D. Sahoo, G. Samanta, and M. De la Sen, "Impact of fear and habitat complexity in a predator-prey system with two different shaped functional responses: a comparative study," *Discrete Dynamics in Nature and Society*, vol. 2021, Article ID 6427864, 22 pages, 2021.
[22] M. L. Rosenzweig, "Exploitation in three trophic levels," *The American Naturalist*, vol. 107, no. 954, pp. 275–294, 1973.
[23] D. J. Wollkind, "Exploitation in three trophic levels: an extension allowing intraspecies carnivore interaction," *The American Naturalist*, vol. 110, no. 973, pp. 431–447, 1976.
[24] S. D. Fretwell, "Food chain dunamics: the central theory of ecology?" *Oikos*, vol. 50, 1987.
[25] P. Panday, N. Pal, S. Samanta, and J. Chattopadhyay, "A three species food chain model with fear induced trophic cascade," *International Journal of Algorithms, Computing and Mathematics*, vol. 5, no. 4, p. 100, 2019.
[26] P. P. Cong, M. Fan, and X. F. Zou, "Dynamics of a three-species food chain model with fear effect," *Communications in Nonlinear Science and Numerical Simulation*, vol. 99, no. 2, Article ID 105809, 2021.
[27] M. Hossain, S. Garai, S. Karmakar, N. Pal, and J. Chattopadhyay, "Impact of vigilance on the density variations in a food chain model," *Ecological Complexity*, vol. 50, Article ID 100996, 2022.
[28] G. Mandal, N. Ali, L. N. Guin, and S. Chakravarty, "Impact of fear on a tri-trophic food chain model with supplementary food source," *International Journal of Dynamics and Control*, vol. 11, no. 5, pp. 2127–2160, 2023.
[29] C. Huang and A. Sih, "Experimental studies on direct and indirect interactions in a three trophic-level stream system," *Oecologia*, vol. 85, no. 4, pp. 530–536, 1991.
[30] H. I. Freedman and P. Waltman, "Mathematical analysis of some three-species food-chain models," *Mathematical Biosciences*, vol. 33, no. 3-4, pp. 257–276, 1977.
[31] M. Hossain, R. Kumbhakar, and N. Pal, "Dynamics in the biparametric spaces of a three-species food chain model with vigilance," *Chaos, Solitons and Fractals*, vol. 162, Article ID 112438, 2022.